August 29, 2012

Volume 51, Number 34

pubs.acs.org/IECR

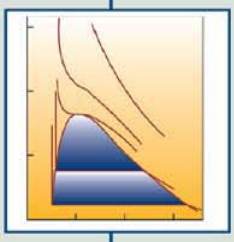

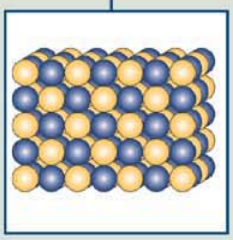

I&EC research

Industrial & Engineering Chemistry Research

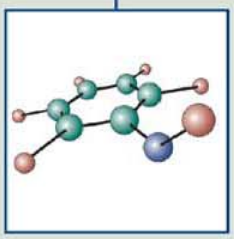

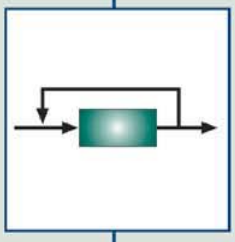

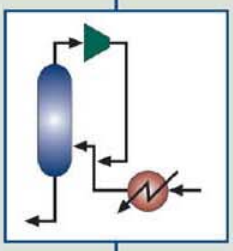

Published by the

American Chemical Society

for Applied Chemistry and

Chemical Engineering

I&EC research
Industrial & Engineering Chemistry Research

Article

pubs.acs.org/IECR

Cost-Effective Production of Pure Al_{13} from $AlCl_3$ by Electrolysis

Wei-Ming Zhang,*[,†] Jin-Xia Zhuang,[†] Qing Chen,[†] Shun Wang,[†] Wei-Guo Song,*[,‡] and Li-Jun Wan[‡]

[†]College of Chemistry & Materials Engineering, Wenzhou University, Wenzhou 325000, P.R. China

[‡]Beijing National Laboratory for Molecular Sciences (BNLMS), Beijing 100190, P.R. China

Supporting Information

ABSTRACT: An integrated electrolysis system was built to synthesize polyaluminum chloride with ultra high-basicity and even pure Al_{13}. The system converts $AlCl_3$ solution from aluminum electrode foil industry waste to Al_{13} chloride directly with reasonable cost, typically \$1.09 per kilogram as $Al_2(OH)_5Cl{\cdot}2H_2O$ at 25 °C. Electrolyte temperature and current density were investigated to optimize the process. Ferron assay and ^{27}Al NMR results indicated that the purity of Al_{13} is over 99% in product solutions. Ion chromatogram analysis confirmed that Cl^- ions accounted for about 96.5% in all counteranions. Our integrated system is the first instance to obtain pure Al_{13} polycations directly. Similar high purity products are only available after tedious purification. This effective and economic synthesis procedure has potential for mass production of Al_{13} for water treatment and catalyst as well as cosmetic industries.

1. INTRODUCTION

China is the largest producer of aluminum electrode foil for electrolytic capacitors. The aluminum electrode foil industry uses HCl to etch the smooth aluminum foil (>99.95% purity) surface and, consequently, produces a large amount of waste acid containing $AlCl_3$. The acid can be recovered by diffusion dialysis (DD),[1,2] while the disposal of the waste solution containing high purity $AlCl_3$ and a small amount of HCl remains an environmental problem. Typically, the $AlCl_3$ solution was neutralized by lime and discharged, which is neither cost-effective nor environmental friendly. It will be very desirable to find a method to convert the waste solution into a highly valuable product at low cost, so that not only waste emission is minimized but also useful product is obtained.

On the other hand, polyaluminum chloride (PAC) has been a very effective material in water treatment. PAC refers to partially neutralized aluminum chloride, defined as $Al_m(OH)_nCl_{3m-n}$, where $m \geq 1$ and $0 < n \leq 3$ m. The neutralization degree, also called basicity of the PAC, is defined by $n/3m$.[3] Aluminum chlorohydrate (ACH), which has an empirical formula of $Al_2(OH)_5Cl{\cdot}2H_2O$, has the highest basicity at ~83%. The dominate Al specie in ACH is Al_{13}: Keggin ε-Al_{13} ($[AlO_4Al_{12}(OH)_{24}(H_2O)_{12}]^{7+}$) polycations.[4,5] Al_{13} is a highly value-added chemical and was widely used as flocculants for potable water and wastewater treatment, catalysts, and cosmetics.[3−21] The latter applications require highly purified Al_{13}.

The conventional synthetic procedure for ACH involves the reaction of pure metallic Al with HCl or $AlCl_3$ solutions at elevated temperature.[3,4] This procedure yields high purity ACH but suffers from high cost of metallic Al and long reaction time (several days or longer). An alternative method for Al_{13} is solution chemistry with elegant reaction setups. Liu and co-workers developed a sophisticated process to inject NaOH into $AlCl_3$ solutions via ultrafiltration (UF) membranes to produce PAC with ~80% Al_{13} with NaCl as the byproduct impurities.[22] Tang et al. developed an electrodialysis (ED) process to substitute anions in $AlCl_3$ solution with OH^- with 2 anion exchange membranes (AEMs), and PAC with ~60% Al_{13} was obtained.[23,24] However, the present commercial AEMs have limited stability in alkali or chlorine solutions because of decomposition. Pratt et al. proposed a process by electrodialysis with bipolar membranes (EDBM).[3] EDBM is a promising method to produce ultra high-basicity PAC and ACH products, with HCl as byproducts. The bipolar membranes are much more expensive compared to conventional ion exchange membranes (IEMs), and their long-term stability is another concern.

The third method to produce PAC and ACH is electrolysis. Typically, metallic Al sheets serve as anodes in $AlCl_3$ or HCl solutions.[10,13,25−28] This process involves electrochemical accelerated reaction of pure metallic Al with HCl or $AlCl_3$ solutions. There are several drawbacks here. First, it is not cost-effective because pure Al metal is involved. Second, the Al anodes are consumables and need frequent replacements, which is not suitable for mass production. An alternative electrolysis process is to use inert electrodes directly.[29,30] Li et al. made related efforts to get PAC with ~91.6% Al_{13} contents.[30]

The above synthesis methods are able to produce PAC with high Al_{13} contents, but none of them are capable of producing pure Al_{13} compounds. Further purification steps such as precipitation, metathesis, UF, or gel-filtration chromatography are needed to produce pure products.[31−36]

In this work, we designed and built an integrated electrolysis system with inert electrodes. The waste solution in the foil industry was a high purity $AlCl_3$ (typically 0.1−1.0 mol/L) solution with low concentration of HCl (typically 1/100−1/10 of $AlCl_3$ concentration). The free HCl can be converted to $AlCl_3$ smoothly by reacting with Al_2O_3 or $Al(OH)_3$ filter cakes, which are available because alkali was used to neutralize the

Received: April 23, 2012
Revised: July 18, 2012
Accepted: August 9, 2012
Published: August 17, 2012

waste acid currently. Thus, pure $AlCl_3$ solution was used as raw material to validate the technology. The unique setup of the electrolysis system enabled us to convert such industry waste solution into pure Al_{13} chloride (over 99%) directly at low costs.

2. EXPERIMENTAL SECTION

2.1. Equipment Setup. The synthesizing system was designed and built on the basis of the National Instruments DAQmx platform. The system diagram was illustrated in Figure 1a. The core module in the system is a home-built electrolytic stack, which is inspired from the design of electrodialysis stacks.[37] The stack consists of a series of titanium electrodes with RuO_2−IrO_2 coatings and PTFE spacers with turbulence nets. The inner configuration of the electrolytic stack was presented in Figure 1b, and the finished stack was shown in Figure 1c. The spacer and electrodes nearby formed an electrolyte flow path. The electrolyte solution was injected by a diaphragm pump (DP-130) and went through the tortuous path in the spacer. The stack contains 12 electrodes and 11 spacers, resulting in 11 parallel flow cells. The DC voltage was applied between the first and last electrodes. Relatively high flow velocity (∼8 cm/s) as well as turbulence nets enhanced the liquid mixing in the stack.

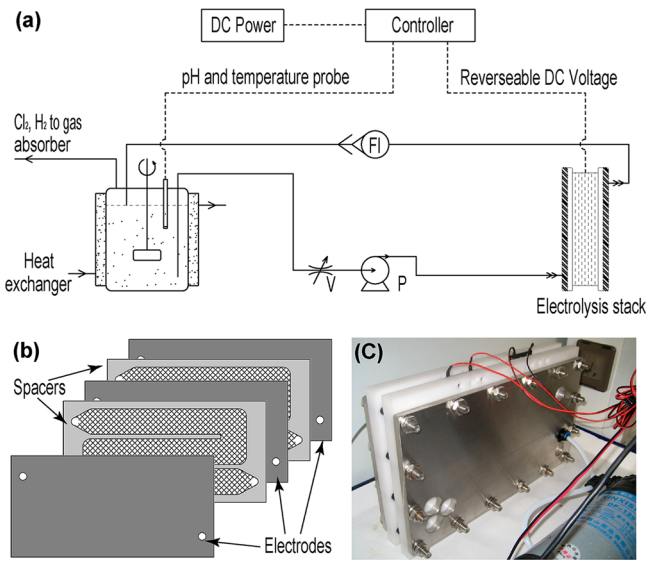

Figure 1. (a) Process diagram of the integrated synthesis system, (b) configurations of the electrolysis stack, and (c) photograph of the electrolysis stack.

2.2. Synthesis Procedures. The system is operated in a batch mode. In a typical operation, 2.0 L of 0.25 mol/L $AlCl_3{\cdot}6H_2O$ (AR, Sinopharm Chemical Reagent Co, Ltd.) aqueous solution was filled in a stirred reaction tank. The temperature of the solution was controlled to 25 ± 1 °C. A 28.5 V DC voltage was applied on the stack. H_2 and Cl_2 gases were generated in the stack and flushed out with the circulating solution. The toxic byproduct Cl_2 gases can be easily eliminated by an alkali scrubber tower in full scale systems, generating disinfectant to compensate the costs. The polarity of the DC voltage was automatically switched every 2 min to avoid aluminum scaling on the electrode surfaces. The stack voltage, current, accumulated charge transfer, and electrolytic solution pH/temperature were recorded simultaneously every 0.5 s. Samples were taken from the reaction tank before and during the electrolysis and then filtrated with a 0.2 μm membrane. All samples and the final products were heated to 70 °C and kept for about 0.5 h before cooling to room temperature to reduce the soluble chlorine in solution.

2.3. Analytical Methods. The total aluminum (Al_t) concentrations were determined by the ferron photometric assay.[38−40] The concentration of ferron is 2.57 mmol/L in the mixed assay solution, and the actual pH is 5.1. The molar ratio of the ferron to the Al_t was kept in the range of 50:1 to 10:1. All standards and samples were mixed with excess dilute HCl (∼20 times of total aluminum concentrations) and heated to 70 °C for 3 h in sealed sample containers, which ensures that the aluminum species are monomer in solutions during the assays.

The Al species distributions of the product samples were analyzed by the timed-photometric assay as well as ^{27}Al NMR spectroscopy.[38−40] Photometric assays were run on a Shimadzu UV-2450 UV−vis spectrophotometer at room temperature, and the absorbance was monitored at 370 nm. The working ferron solution was identical to Al_t determination. ^{27}Al NMR was run on a Bruker Avance-III 500 spectrometer at room temperature. A mixing aqueous solution with 0.25 mL of D_2O and a 0.25 mL sample was used in the experiment. A 0.125 mol/L $AlCl_3$ solution with 50% of D_2O was used as reference for 0 ppm. Ion chromatogram (DIONEX ICS-1000) was also employed to analyze the anions in the samples, and the testing details can be found in Supporting Information.

3. RESULTS AND DISCUSSION

3.1. Data Profiles during the Electrolysis Reaction. A typical current profile recorded by the system was presented in Figure 2a. The polarity of the DC voltage changed every 2 min to eliminate the scaling risks, and extra 1 min intervals of rest were added after each polarity switching. During the rest intervals, pH can be measured without interference by the DC electric field of electrolysis. The rest intervals can be shortened or even eliminated with limited precision lost. There are current spikes (as high as 6 A) during DC polarity changes,

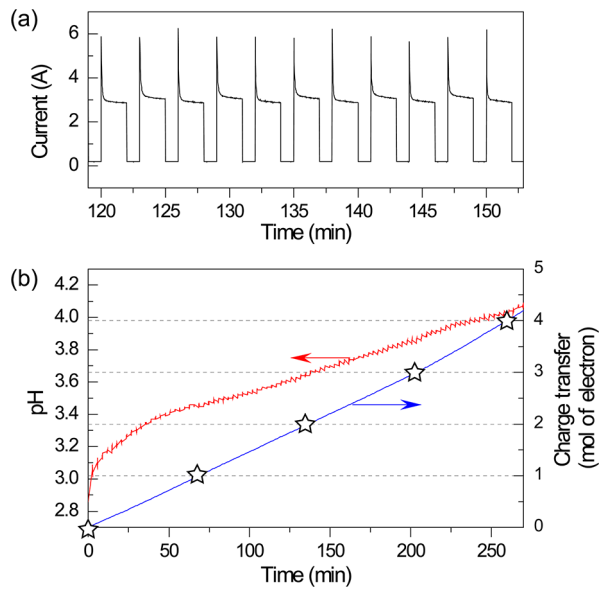

Figure 2. Data profiles during the electrolysis process: (a) current curves; (b) pH profile and charge transfer curves. The sampling points are marked with a ☆, respectively, from sample A to E.

Table 1. Analysis Results of All Samples

sample index	charge transfer (mol of electron)	pH	Al_t (mol/L)	Al_a, %	Al_b, %	Cl^- (mol/L)	ClO_3^- (mol/L)	basicity, %
A	0.0	2.86	0.254	100.0	0.0	0.749	$<10^{-3}$	0.1
B	1.0	3.44	0.250	80.1	19.9	0.486	$<10^{-3}$	35.2
C	2.0	3.66	0.246	27.8	72.2	0.269	1.4×10^{-3}	64.9
D	3.0	3.86	0.251	0.8	99.2	0.154	5.3×10^{-3}	78.4
E	4.0	4.04	0.249	0.4	99.6	0.124	1.62×10^{-2}	81.8

which originated from the electrochemical capacitance of the electrodes. Then, the current fell and stabilized at about 2.8 A. The polarity switch is essential to ensure the stability of the synthesis process.

The normalized cell voltage is 2.60 V for each cell (28.5 V for 11 cells), which is close to the theoretical deposition voltage of 2.21 V. The effective area of the electrodes is 140 cm^2; thus, the current density during the electrolysis is 20 mA/cm^2. The cell voltage in this study is much lower than those in previous reports (typically 6−18 V for comparable current density),[25−27,29,30] leading to higher energy efficiency of the synthesis process. The stack design in this study has several advantages. First, the electrode distance in our stack is only 0.6 mm, resulting in a very small ohmic voltage drop; and the insulating PTFE spacer eliminated the risk of short circuit. The distance between electrodes in previous works is typically 10−30 mm, and the voltage drop on ohmic resistance of the electrolyte is relatively high. Second, tortuous turbulence accelerating spacers (common in commercial ED stacks, detailed spacer design presented in Figure 1b)[37] were employed to eliminate the concentration polarization, which caused considerable superpotential during the electrolysis process.

The following electrolytic reactions occurred on the electrode surfaces.

$$\text{Anode: } 2Cl^- \rightarrow Cl_2 + 2e^- \quad (1)$$

$$\text{Cathode: } 2H_2O + 2e^- \rightarrow H_2 + 2OH^- \quad (2)$$

The net result of the electrolytic process is to substitute Cl^- ions with OH^- ions in $AlCl_3$ solution. The Al^{3+} reacted with the yielded OH^- ions to produce Al_{13} polycations. The Al speciation during the electrolysis is very similar to that of metallic Al [4] as well as the base-injecting[22] method. Briefly, the $[Al(H_2O)_6]^{3+}$ ions hydrolyze and produce $[Al(OH)_2(H_2O)_4]^+$ ions or $[Al_2(OH)_4(H_2O)_6]^{2+}$ dimers first as the Cl^- is substituted by OH^- in the electrolysis reaction. At the same time, the local high hydroxyl concentration close to the cathode has a good chance for initial tetrahedral $Al(OH)_4^-$ formation. The tetrahedral $Al(OH)_4^-$ migrates away from the cathode and coordinates with 12 $[Al(OH)_2(H_2O)_4]^+$ or 6 $[Al_2(OH)_4(H_2O)_6]^{2+}$ quickly to form Al_{13} polycation via hydroxyl bridges.[4,22] The enhanced mixing in the stack as well as the polarity switching abates the $Al(OH)_3$ formation, which are helpful for Al_{13} production.

The pH of electrolyte solution increased during the reaction, which is shown in Figure 2b. Five samples were collected when charge transfer reached 0, 1, 2, 3, and 4 mol of electron, respectively. The sampling points were marked with star symbols (☆) in Figure 2b, and labeled as samples A, B, C, D, and E, respectively.

3.2. Evolution of Al Species Distribution. Total aluminum (Al_t) concentrations of all samples were determined by photometric assays, and the results are shown in Table 1. The Al_t is constant (0.25 mol/L) during the electrolysis, indicating that there was little Al scaling generated on the electrode surfaces.

The main Al species in neutralized solutions can be classified into three catalogues: Al_a (mononuclear Al), Al_b (reactive polynuclear Al_{13}), and Al_c (mainly Al colloids). Timed-photometric assays of ferron are widely used to analyze the distribution of Al species in partially neutralized Al solutions.[38−40] The stacked curves of the timed-photometric assays are presented in Figure 3a. Initial absorbance of the assay

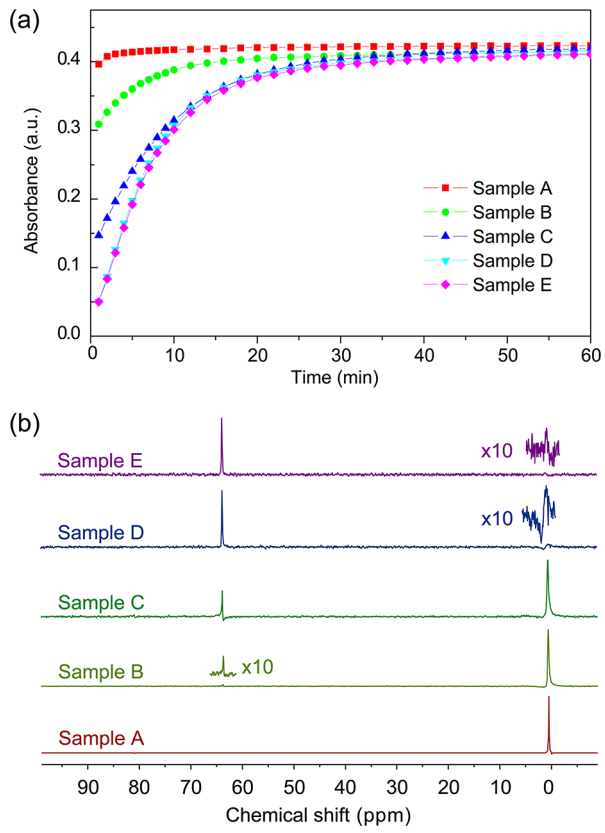

Figure 3. Analysis of Al species distributions in samples. (a) Absorbance curves of time-photometric ferron assays. (b) ^{27}Al NMR spectrum of the samples. Parts of the spectra at 0 and 63.5 ppm were enlarged 10 times to highlight the presence of small peaks.

solution is related to the Al_a species, the absorbance increment during the assay is related to Al_b concentration, and Al_c concentration can be calculated by Al_t. Sample A is initial acidic $AlCl_3$ solution with no Al_b or Al_c in it. The initial absorbance is 0.39, and the final absorbance is 0.42. The final absorbances of all other samples are nearly the same, confirming that there are no Al_c either in theses samples. Meanwhile, the initial absorbance of samples B, C, D, and E decrease dramatically, which means Al_a concentrations decreased while Al_b concentrations increased. For samples D and E, the assay curves are nearly identical, indicating that the

Al species distribution is stable during that period. There are nearly no Al_a in these two samples as the extrapolated absorbance is nearly 0 at 0 min.

^{27}Al NMR is another widely used method to evaluate the Al species distribution.[4,26,41] The structure configurations of Al atoms in Al_a and Al_b species are different in aqueous solution and distinguishable in ^{27}Al NMR spectra. The Al atoms of Al_a species are in octahedral environments, corresponding to a chemical shift of 0 ppm. The Al_{13} polycation has a Keggin structure, containing a central Al atom in a tetrahedral environment (63.5 ppm) surrounded by 12 Al atoms in octahedral environments (no signal in this configuration). The concentration ratio of Al_a and Al_b can be obtained from the intensities of 0 ppm and 63.5 ppm resonances in the spectra.[42] The ^{27}Al NMR spectra of all samples are shown in Figure 3b. For sample A, the absence of 63.5 ppm signal confirmed that all Al atoms are in octahedral environments. As the electrolysis reaction began, the 63.5 ppm resonance increased and the 0 ppm resonance decreased. The concentration ratios of Al_a and Al_b for all samples were calculated from the relative intensities of 0 ppm peak and 63.5 ppm peak. The final Al species distributions are determined and shown in Table 1. All Al atoms in electrolyte solution were converted to Al_{13} Keggin structures after the charge transfer reached 3 mol electrons, resulting in Al_{13} with over 99% purity.

Direct synthesis of pure Al_{13} polycations is extremely difficult. The Al_a signals in the ^{27}Al NMR spectrum exist even in high purity ACH product synthesized by the metallic Al oxidation method.[4] To produce pure Al_{13} products, tedious purification steps are frequently used.[31−36] For example, Shi et al. proposed a method to separate pure Al_{13} contents from PAC solutions by sulfate precipitation and nitrate metathesis.[31] Their purified products have a similar NMR spectrum as samples D and E. The integrated system and electrolysis procedure in this study are a direct and simple method to produce pure Al_{13} polycations, and the counteranion is Cl^-, which is desirable for practical applications.

3.3. Byproduct Anions and Side Reactions. Side reactions and byproduct are involved in most electrolysis processes. Specifically ClO^-, ClO_2^-, ClO_3^-, and ClO_4^- are possible byproduct anions in this study. High value-added applications such as deodorant and antiperspirant usually are very sensitive to these impurities, so it is important to figure out the levels of these anions. In this synthesis process, the pH of product solutions is slightly acidic (pH 3.5−4.0), so the ClO^- ions hardly exist since HClO ($K_\alpha = 3.4 \times 10^{-8}$) is a very weak acid. An ion chromatogram method was used to analyze the ClO_2^-, ClO_3^-, and ClO_4^- byproduct anions as well as Cl^- in all samples. The anion chromatogram spectra were presented in Figure S1 in Supporting Information. Parts of the Cl^- ions were oxidized and converted to Cl_2 gases, getting out of the reactor, so the concentration of Cl^- ions decreased remarkably during the electrolysis process. In all samples, ClO_2^- and ClO_4^- ions were not detected, while trace ClO_3^- ions were found. The concentration of the ClO_3^- ions increased during the reaction. The quantitative analysis results of the anions in the samples are listed in Table 1. The concentration of impurity anions is quite low compared to Cl^- ions. For sample D, the concentration of impurity ClO_3^- anions accounted for 3.5% of anions, and the Al_{13} contents are as high as 99.2%, which should be sufficient even for cosmetics.

3.4. Evolution of Product Basicity. The basicity of the samples can be determined via the concentrations of total Al and the Cl^-/ClO_3^- ions by the following formula:

$$\text{Basicity} = \frac{[OH^-]'}{3[Al_t]} = \frac{[Cl^-]_0 - [Cl^-] - [ClO_3^-]}{3[Al_t]} \quad (3)$$

where $[OH^-]'$ is the concentration of the generated hydroxyl groups; $[Al_t]$ is the total Al concentration in solution; $[Cl^-]_0$ is the initial concentration of Cl^-; $[Cl^-]$ and $[ClO_3^-]$ are the detected concentrations of Cl^- and ClO_3^- ions, respectively. In this study, $[Al_t]$ and $[Cl^-]_0$ are 0.25 mol/L and 0.75 mol/L, respectively. As listed in Table 1, the basicity of samples D and E are very close to the theoretical basicity of pure Al_{13} chloride ($AlO_4Al_{12}(OH)_{24}(H_2O)_{12}Cl_7$, basicity = 82%), confirming that highly pure Al_{13} products were produced directly.

3.5. Current Efficiency and Cost Estimation. The optimum reaction end point is sample D for the synthesis process in this study, resulting in a current efficiency of about 41%. The current efficiency was lowered due to the side reactions involved in the electrolysis process. First, O_2 gases are generated on anodes from the water dissociation reaction, which is useless for Al_{13} production. The Ti electrodes with RuO_2−IrO_2 coating were chosen in this study because of its low superpotential for Cl_2, so the amount of O_2 generated is limited when the concentration of Cl^- is relatively high. Second, the generated H_2 and Cl_2 gases may migrate to the counter electrode surfaces, and the following electrolytic reactions may occur:

$$\text{Anodes: } H_2 - 2e^- \rightarrow 2H^+ \quad (4)$$

$$\text{Cathodes: } Cl_2 + 2e^- \rightarrow 2Cl^- \quad (5)$$

These side reactions are reverse of the main electrolytic reactions, significantly lowering the current efficiency (eqs 1 and 2). Anion exchange membranes (AEMs) resistant to strong oxidants as well as alkali may be used to significantly increase the current efficiency.

The cell voltage in the electrolysis stack is quite low compared to previous reports. Figure 4a presents the cell voltage vs current density curves of the stack at 5, 25, and 55 °C, respectively. For instance, at 25 °C, the current density is 18 mA/cm^2 with a cell voltage of 2.6 V and increased to 45 mA/cm^2 with a cell voltage of 3.0 V.

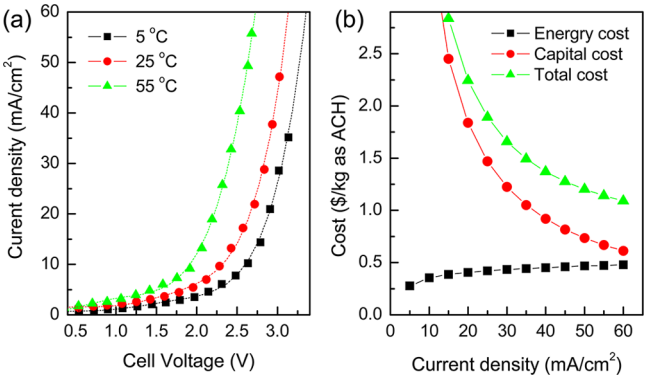

Figure 4. (a) Current density vs cell voltage curves of the stack at different temperatures; the electrolytes are 0.25 mol/L $AlCl_3$ for all tests. (b) Cost estimation of the electrolysis process at 25 °C.

The current density and energy consumption increases as the cell voltage rises, while many more products can be produced, so the capital cost decreases. There is a trade-off for current density. Table 2 lists part of the parameters to estimate the costs for the synthesis procedure, and the corresponding results are shown in Figure 4b. Details of the cost estimation were described in the Supporting Information. The energy cost increases slowly, and the capital cost decreases swiftly as the current density increases. The total cost decrease as the current density increases within the range from 5 to 60 mA/cm^2 tested in this study, and no inflection is observed, indicating that the most cost-effective current density may be higher than 60 mA/cm^2. The optimal current density is not observed because of the output limitation of the DC power supply used in this study. The minimum cost is thus estimated at 60 mA/cm^2, which is about \$1.09 for 1 kg of Al_{13} products (calculated as ACH, \$0.48 for energy cost and \$0.61 as capital cost) at 25 °C.

Table 2. Parameters for the Cost Estimation of Electrolysis Process

parameters	electrolysis process	remarks
current efficiency (%)	41	
operation temperature (°C)	25	
anode electrode price (\$/m^2)	500	
cathode electrode price (\$/m^2)	500	
electrode area (m^2)	10	
effective electrode area (m^2)	8	
stack cost (\$)	15 000	1.5 times electrode cost
peripheral equipment cost (\$)	15 000	same as stack cost
total investment cost (\$)	30 000	
amortization (\$/year)	10 000	3 years
interest (\$/year)	2400	8% interest rate
maintenance (\$/year)	3000	10% investment cost
total capital cost (\$/year)	15 400	
electricity charge (\$/kWh)	0.10	

It is also suggested in Figure 4a that high electrolyte temperature is favorable to reduce the cell voltage, so it is helpful to reduce the energy cost by heating the electrolyte solution during the electrolysis. The minimum cost is \$1.03 for 1 kg of Al_{13} products as ACH at 55 °C.

4. CONCLUSION

China has become the largest producer of aluminum electrode foil for electrolytic capacitors, the global demand of which has grown steadily and rapidly. A large amount of concentrated HCl solution (normally 6 M) was used in the etching process to generate porous structure on the smooth aluminum foil surface, and consequently, a large amount of waste acid containing $AlCl_3$ was produced. The waste HCl was usually recovered by DD.[2] The remaining solution contained high purity $AlCl_3$ and a small amount of HCl and has been an environmental concern for the aluminum electrode foil industry and environmental regulators. Typically, the $AlCl_3$ solution was neutralized by lime and discharged. This is by no means a satisfactory solution. Thus, the benefit of this technique is 2-fold. First, industry waste emission can be minimized since effluent after DD can be readily treated. Second, a highly valuable environmental protection product, Al_{13}, was produced directly at low cost.

■ ASSOCIATED CONTENT

Supporting Information

Details of cost estimation and supplementary figure on separation of anions in samples by ion chromatogram. This material is available free of charge via the Internet at http://pubs.acs.org.

■ AUTHOR INFORMATION

Corresponding Author

*E-mail: weiming@iccas.ac.cn (W.-M.Z.); wsong@iccas.ac.cn (W.-G.S.).

Notes

The authors declare no competing financial interest.

■ ACKNOWLEDGMENTS

The authors are grateful for financial support from the National Natural Science Foundation of China (Project No. 21003097) and the Natural Science Foundation of Zhejiang Province (Project No. Y4100515).

■ REFERENCES

(1) Luo, J.; Wu, C.; Xu, T.; Wu, Y. Diffusion dialysis-concept, principle and applications. *J. Membr. Sci.* **2011**, *366* (1−2), 1−16.

(2) Zhang, X.; Li, C.; Wang, H.; Xu, T. Recovery of hydrochloric acid from simulated chemosynthesis aluminum foil wastewater by spiral wound diffusion dialysis (SWDD) membrane module. *J. Membr. Sci.* **2011**, *384* (1−2), 219−225.

(3) Pratt, W. E.; Stevens, J. J.; Symons, P. G. Polyaluminum chloride and aluminum chlorohydrate, processes and compositions: High-basicity and ultra high-basicity products. US Patent 7,846,318, Dec. 7, 2010.

(4) Teagarden, D. L.; Hem, S. L.; White, J. L. Conversion of aluminum chlorohydrate to aluminum hydroxide. *J. Soc. Cosmet. Chem.* **1982**, *33*, 281−295.

(5) Casey, W. H. Large aqueous aluminum hydroxide molecules. *Chem. Rev.* **2006**, *106* (1), 1−16.

(6) Can, O. T.; Bayramoglu, M.; Kobya, M. Decolorization of reactive dye solutions by electrocoagulation using aluminum electrodes. *Ind. Eng. Chem. Res.* **2003**, *42* (14), 3391−3396.

(7) Duan, J.; Gregory, J. Coagulation by hydrolysing metal salts. *Adv. Colloid Interface Sci.* **2003**, *100−102* (0), 475−502.

(8) Matsui, Y.; Matsushita, T.; Sakuma, S.; Gojo, T.; Mamiya, T.; Suzuoki, H.; Inoue, T. Virus inactivation in aluminum and polyaluminum coagulation. *Environ. Sci. Technol.* **2003**, *37* (22), 5175−5180.

(9) Barrera-Diaz, C.; Roa-Morales, G.; Avila-C0rdoba, L.; Pavon-Silva, T.; Bilyeu, B. Electrochemical treatment applied to food-processing industrial wastewater. *Ind. Eng. Chem. Res.* **2005**, *45* (1), 34−38.

(10) Canizares, P.; Carmona, M.; Lobato, J.; Martinez, F.; Rodrigo, M. A. Electrodissolution of aluminum electrodes in electrocoagulation processes. *Ind. Eng. Chem. Res.* **2005**, *44* (12), 4178−4185.

(11) Gao, B.-Y.; Chu, Y.-B.; Yue, Q.-Y.; Wang, B.-J.; Wang, S.-G. Characterization and coagulation of a polyaluminum chloride (PAC) coagulant with high Al13 content. *J. Environ. Manage.* **2005**, *76* (2), 143−147.

(12) Hu, C.; Liu, H.; Qu, J.; Wang, D.; Ru, J. Coagulation behavior of aluminum salts in eutrophic water: Significance of Al13 species and pH control. *Environ. Sci. Technol.* **2006**, *40* (1), 325−331.

(13) Canizares, P.; Jimenez, C.; Martinez, F.; Saez, C.; Rodrigo, M. A. Study of the electrocoagulation process using aluminum and iron electrodes. *Ind. Eng. Chem. Res.* **2007**, *46* (19), 6189−6195.

(14) Shi, B.; Li, G.; Wang, D.; Feng, C.; Tang, H. Removal of direct dyes by coagulation: The performance of preformed polymeric aluminum species. *J. Hazard. Mater.* **2007**, *143* (1−2), 567−574.

(15) Wu, X.; Ge, X.; Wang, D.; Tang, H. Distinct coagulation mechanism and model between alum and high Al13-PACl. *Colloids Surf., A* **2007**, *305* (1−3), 89−96.
(16) Lin, J.-L.; Chin, C.-J. M.; Huang, C.; Pan, J. R.; Wang, D. Coagulation behavior of Al13 aggregates. *Water Res.* **2008**, *42* (16), 4281−4290.
(17) Wu, X.; Wang, D.; Ge, X.; Tang, H. Coagulation of silica microspheres with hydrolyzed Al(III) - Significance of Al13 and Al13 aggregates. *Colloids Surf., A* **2008**, *330* (1), 72−79.
(18) Zhao, H.; Hu, C.; Liu, H.; Zhao, X.; Qu, J. Role of aluminum speciation in the removal of disinfection byproduct precursors by a coagulation process. *Environ. Sci. Technol.* **2008**, *42* (15), 5752−5758.
(19) Gu, Z.; Liao, Z.; Schulz, M.; Davis, J. R.; Baygents, J. C.; Farrell, J. Estimating dosing rates and energy consumption for electrocoagulation using iron and aluminum electrodes. *Ind. Eng. Chem. Res.* **2009**, *48* (6), 3112−3117.
(20) Stewart, T. A.; Trudell, D. E.; Alam, T. M.; Ohlin, C. A.; Lawler, C.; Casey, W. H.; Jett, S.; Nyman, M. Enhanced water purification: A single atom makes a difference. *Environ. Sci. Technol.* **2009**, *43* (14), 5416−5422.
(21) Xu, W.; Gao, B.; Wang, Y.; Yang, Z.; Bo, X. Role of Al13 species in removal of natural organic matter from low specific UV absorbance surface water and the aggregates characterization. *Chem. Eng. J.* **2011**, *171* (3), 926−934.
(22) Jia, Z.; He, F.; Liu, Z. Synthesis of polyaluminum chloride with a membrane reactor: Operating parameter effects and reaction pathways. *Ind. Eng. Chem. Res.* **2003**, *43* (1), 12−17.
(23) Qu, J.; Lu, G.; Tang, H. Synthesis of polyaluminum chloride by electrodialysis. CN Patent 1,186,773, Jul. 8, 1998.
(24) Lu, G.; Qu, J.; Tang, H. Study on the highly effective synthesis of polyaluminum chloride by electrodialysis. *Environ. Sci. (China)* **2000**, *20* (3), 250−253.
(25) Lu, G.; Qu, J.; Tang, H. The electrochemical production of highly effective polyaluminum chloride. *Water Res.* **1999**, *33* (3), 807−813.
(26) Qu, J.; Liu, H. Optimum conditions for Al13 polymer formation in PACl preparation by electrolysis process. *Chemosphere* **2004**, *55* (1), 51−56.
(27) Pi, K. W.; Gao, L. X.; Li, Z.; Wang, M.; Huang, L. PAC with high content of Al13 polymer prepared by electrolysis with periodical reversal of electrodes. *Colloids Surf., A* **2011**, *387* (1−3), 113−117.
(28) Liu, H.-J.; Qu, J.-H.; Hu, C.-Z.; Zhang, S.-J. Characteristics of nanosized polyaluminum chloride coagulant prepared by electrolysis process. *Colloids Surf., A* **2003**, *216* (1−3), 139−147.
(29) Hu, C.; Liu, H.; Qu, J. Preparation and characterization of polyaluminum chloride containing high content of Al13 and active chlorine. *Colloids Surf., A* **2005**, *260* (1−3), 109−117.
(30) Li, X.-Z.; Ye, Q.-F.; Wang, L.-J. Polyaluminum chloride with high Al13 content rapidly prepared by electrolysis with exchanging electrodes. *J. Inorg. Mater. (China)* **2007**, *22* (6), 1211−1215.
(31) Shi, B.; Li, G.; Wang, D.; Tang, H. Separation of Al13 from polyaluminum chloride by sulfate precipitation and nitrate metathesis. *Sep. Purif. Technol.* **2007**, *54* (1), 88−95.
(32) Lin, Y.-F.; Lee, D.-J. Purification of aluminum tridecamer salt using organic solvent precipitation. *Sep. Purif. Technol.* **2010**, *75* (2), 218−221.
(33) Huang, L.; Wang, D.; Tang, H.; Wang, S. Separation and purification of nano-Al13 by UF method. *Colloids Surf., A* **2006**, *275* (1−3), 200−208.
(34) Guo, Y.; Li, G.; Zhao, C.; Zhao, Q.; Wang, J.; Luan, Z. High-concentration ε-Al13 nanoclusters sol prepared by chemical synthesis and membrane distillation concentration process. *Sep. Purif. Technol.* **2009**, *69* (2), 221−223.
(35) Gao, B.; Chu, Y.; Yue, Q.; Wang, Y. Purification and characterization of Al13 species in coagulant polyaluminum chloride. *J. Environ. Sci.* **2009**, *21* (1), 18−22.
(36) Chu, Y.; Gao, B.; Yue, Q.; Wang, Y.; Wang, S. Characterization and separation of Al13 species using gel-filtration chromatography. *Sci.China Ser. B* **2006**, *49* (4), 326−331.
(37) Strathmann, H. Electrodialysis, a mature technology with a multitude of new applications. *Desalination* **2010**, *264* (3), 268−288.
(38) Jardine, P. M.; Zelazny, L. W. Mononuclear and polynuclear aluminum speciation through differential kinetic reactions with ferron. *Soil. Sci. Soc. Am. J.* **1986**, *50*, 895−900.
(39) Parker, D. R.; Bertsch, P. M. Identification and quantification of the "Al13" tridecameric aluminum polycation using ferron. *Environ. Sci. Technol.* **1992**, *26* (5), 908−914.
(40) Wang, C.-Y.; Zhang, C.-H.; Bi, S.-P.; Zhang, Z.-C.; Yang, W.-H. Assay of three kinds of aluminum fractions (Ala, Alb and Alc) in polynuclear aluminum solutions by Al-ferron timed spectrophotometry and demarcation of their time limits. *Spectrosc. Spect. Anal. (China)* **2005**, *25*, 252−256.
(41) Allouche, L.; Gérardin, C.; Loiseau, T.; Férey, G.; Taulelle, F. Al30: A giant aluminum polycation. *Angew. Chem., Int. Ed.* **2000**, *39* (3), 511−514.
(42) Bottero, J. Y.; Axelos, M.; Tchoubar, D.; Cases, J. M.; Fripiat, J. J.; Fiessinger, F. Mechanism of formation of aluminum trihydroxide from keggin Al13 polymers. *J. Colloid Interface Sci.* **1987**, *117* (1), 47−57.

Supporting Information for

"Cost-effective Production of Pure Al_{13} from $AlCl_3$ by Electrolysis"

Wei-Ming Zhang[1], Jin-Xia Zhuang[1], Qing Chen[1], Shun Wang[1], Wei-Guo Song*[2] and Li-Jun Wan[2]*

[1] College of Chemistry & Materials Engineering, Wenzhou University, Wenzhou 325000, P.R. China

[2] Beijing National Laboratory for Molecular Sciences (BNLMS), Beijing 100190, P.R. China

*Corresponding author. E-mail: weiming@iccas.ac.cn, wsong@iccas.ac.cn

Details of cost estimation

The technology readiness level (TRL) of this work still stays low (TRL 4 at present), it is hard to calculate the cost precisely at this stage. So rough cost estimation is given in this study.

The process cost is estimated according to quotations from DSA vendors, experimental data as well as project experiences. All parameters and reasoning are presented in table 2. For a stack with 10 m^2 cathode and anode areas, the effective electrode areas maybe 20% less because the sealing takes up some areas. The stack consists of electrodes, spacers, endplates and et al. The majority of cost is electrode, and the cost of other stack components take approximately 50% of electrode, so the total cost of the stack is ($500*10+$500*10)*150%=$15000. We also need auxiliary equipments such as pumps, piping systems, DC rectifier, degasifier, tank, mixer, PLC and et al. The cost of these peripheral equipments should be another $15000 according to previous experiences. Therefore an investment of $30000 is needed to setup a system with 8 m^2 effective electrode areas. Typically the capital investment is amortized during the lifespan to reduce the cash flow for industrial projects. The materials which

directly contact with the solutions are carefully selected for well chemical resistance in system design, so the 3-year lifespan is achievable for the system. In these 3 years, we must pay extra $2400 interest to the bank each year at 8% interest rate. In addition, daily maintenance and human labor are needed to ensure the proper operation of the system, which is 10% of total capital investment per year. It means that in the 3-year lifespan, we need pay $10000 (1/3 of investment) + $2400 (interest for amortization) + $3000 (maintenance) = $15400 per year. The operation time typically is 8000 hours per year in industry, so the production of Al_{13} can be calculated by current density, current efficiency, electrode area as well as time. For example, the annual Al_{13} production as ACH at 60 mA/cm^2 was calculated as following:

$$\frac{600A/m^2 \times 8m^2 \times 8000h \times 3600s/h}{\frac{1000g/kg \times 2.46 \times 2}{41\% \times 210.5g/mol(\mathrm{ACH})} \times 96485C/mol} = \frac{1.38 \times 10^{11} C}{5.50 \times 10^6 C/kg} = 2.51 \times 10^4 kg$$

We know that the annual capital cost was $15400, so the capital cost is $15400/25100 kg = $0.61 per kg as ACH.

Similarly, the energy cost can be calculated by the cell voltage (presented in Figure 4a) and current efficiency. For example, the energy cost (mainly electrolysis) at 60 mA/cm^2 (cell voltage is 3.13V) was calculated as following:

$$3.13V \times \frac{1000g/kg \times 2.46 \times 2}{41\% \times 210.5g/mol(\mathrm{ACH})} \times 96485C/mol = 1.72 \times 10^7 J/kg$$
$$= 4.78kWh/kg$$

The charge of the industrial electricity is $0.10/kWh, which also listed in table 2. So the energy cost is $0.48 per kg as ACH.

The cost model is fully base on parameters in table 2. The capital costs as well as energy costs at different current densities are all calculated by the cost model computer program, and presented in Figure 4b.

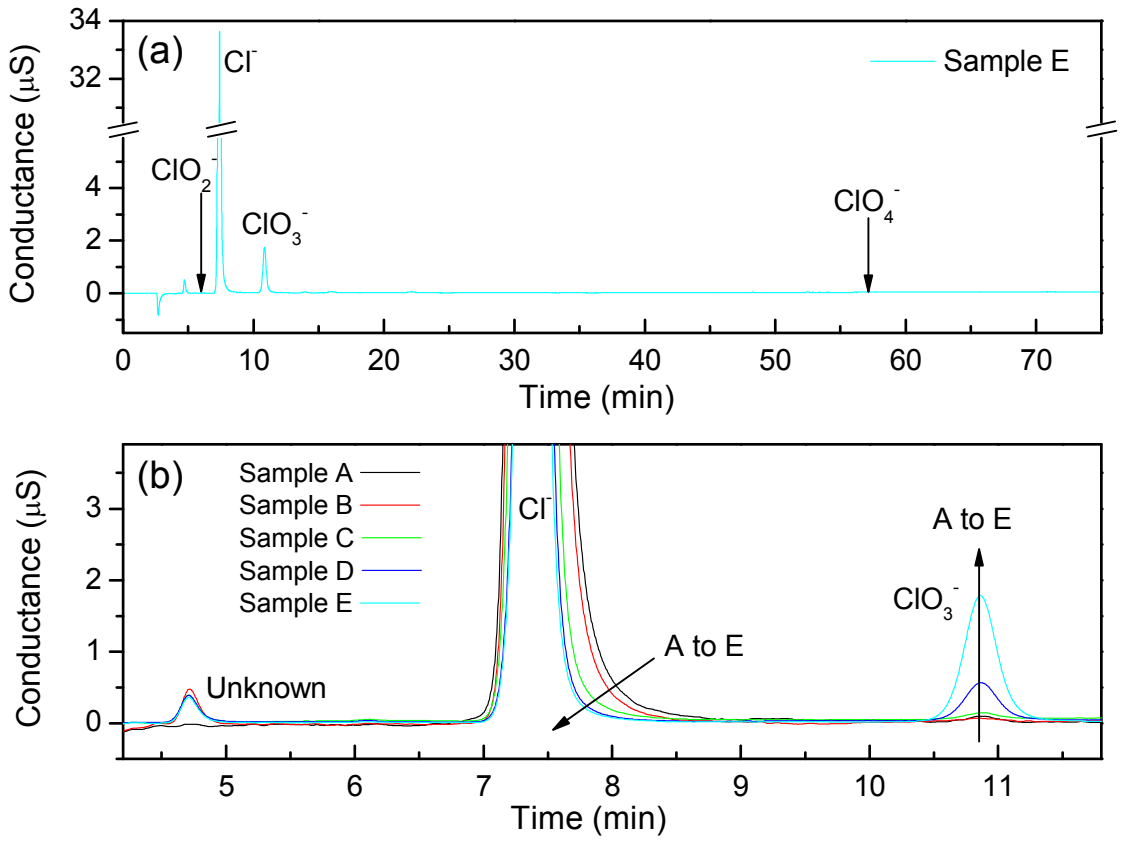

Figure S1. Separation of anions in samples by ion chromatogram. a) full-scale spectrum of sample E and b) closed look of all samples. Ion chromatogram (DIONEX® ICS-1000) was employed to analyze the anions in the samples under the following conditions: column, Dionex® IonPac® AS23 (4 mm); eluent, 4.5 mM Sodium carbonate/0.8 mM Sodium bicarbonate; flow rate, 1.0 mL/min; detection, suppressed conductivity with an anion self-regenerating suppressor (ASRS) operated at 25 mA in recycle mode; injection volume, 25 μL; temperature: 35 °C. The samples were diluted 100-500 times with deionized water before the analysis.